Prompt fission neutron investigations with position sensitive detector

Sh. Zeynalov, O.V. Zeynalova, P. Sedyshev , V. Shvetsov and V. Smirnov

Joint Institute for Nuclear Research, Dubna, Russia

Motivation

Experiments with simultaneous measurement of FF, kinetic energies, mass and the FF emission angle in coincidence with PFN emission provides valuable data characterizing the dynamic of fission process. The quality of experimental data was significantly elaborated recently by application of digital pulse processing.

In our previous works we have introduced digital pulse processing, implemented for 252Cf(SF) reaction investigation. There were demonstrated two most essential advantages of DPP over conventional analog electronics:

- **The possibility of repeated analysis of the same data set with a different pulse processing algorithms.**
- **Much higher precision of measured data (in terms of the pulse height resolution) and the diversity of information became available thanks to digital pulse processing**

The next modification of the method was intended to overcome the limitation of the method by increasing the PFN detection efficiency by adding neutron detectors allocated in most efficient way around the FF detector. Such modification will improve the quality of experiments with targets of "non zero thickness" like ^{239}Pu, ^{235}U and so on.

PFN emission kinematics in double E experiment

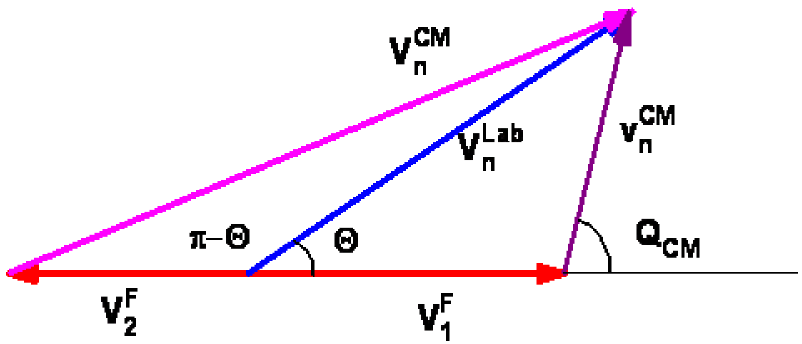

The detailed information on PFN emission in fission is available from the measured dependence of average number of PFN emitted by the FF with mass number A and the TKE release of two fission fragments.

$$\bar{\nu}(A) = \frac{\int_0^\infty \bar{\nu}(A,TKE)Y(A,TKE)dTKE}{\int_0^\infty Y(A,TKE)dTKE} \text{ or } \bar{\nu}(TKE) = \frac{\int_0^\infty \bar{\nu}(A,TKE)Y(A,TKE)dA}{\int_0^\infty Y(A,TKE)dA}$$

$$\bar{\nu} = \int_0^\infty \bar{\nu}(A,TKE)Y(A,TKE)dTKEdA, \quad 200 = \int_0^\infty Y(A,TKE)dTKEdA$$

DPP electronics for PFN investigation

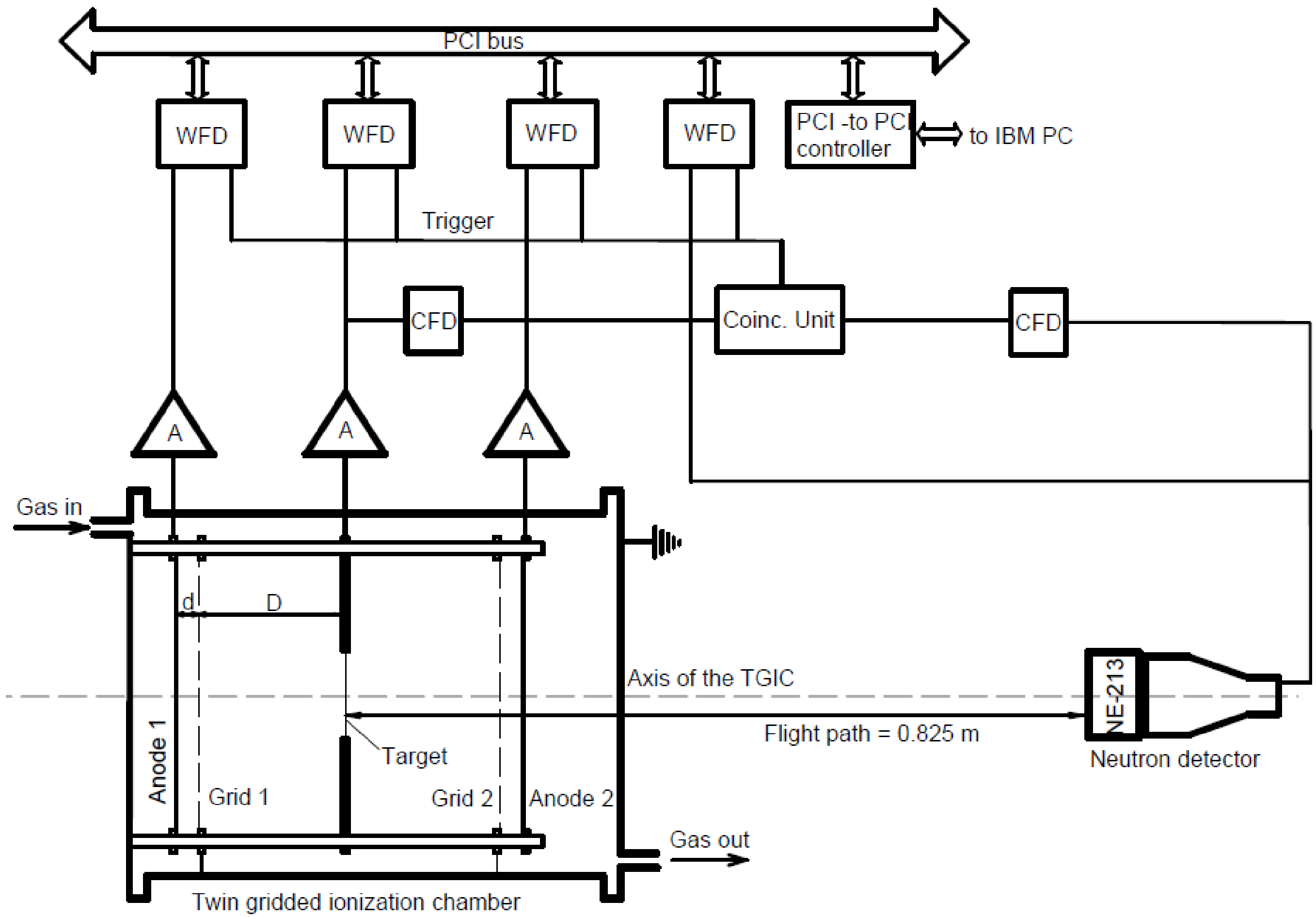

Prompt fission neutron investigation

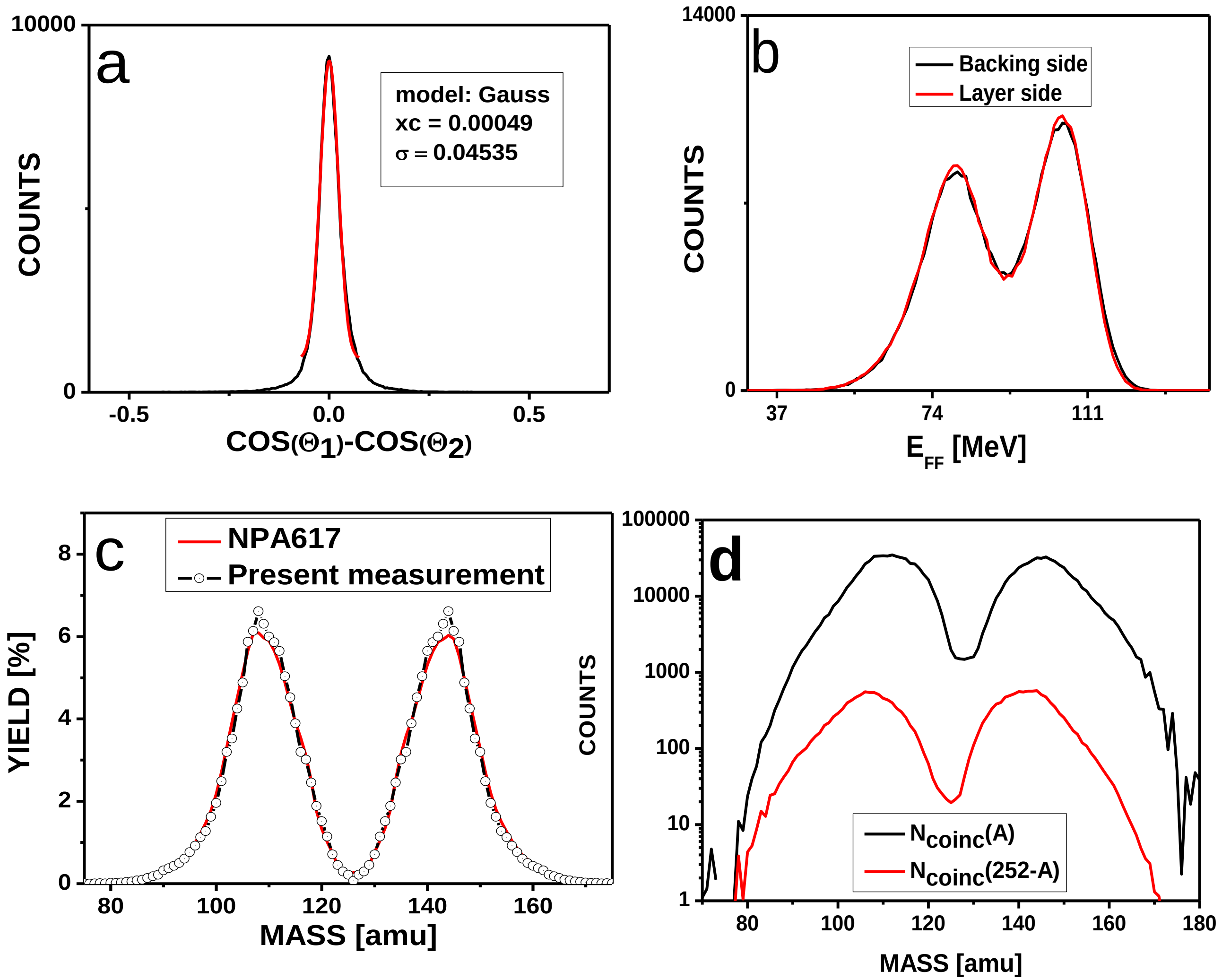

Prompt fission neutron investigation

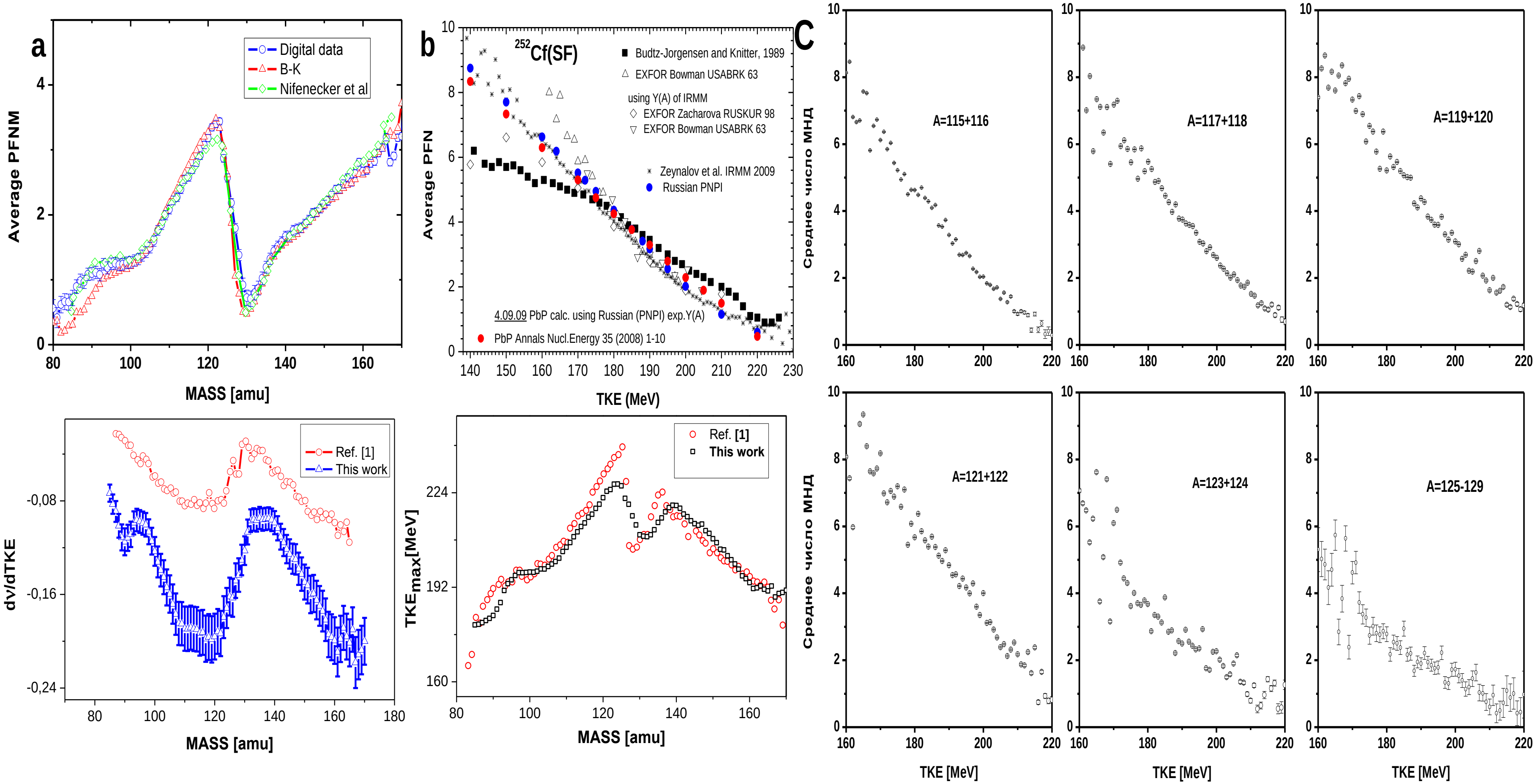

Average PFN multiplicity dependence on mass split and TKE obtained from measured matrix $\nu(A,TKE)$, integrated over A or TKE. On the right side average PFN multiplicity plotted versus TKE for the selected mass regions, indicated on the plot. These plots were used to calculate the slopes and maximum value of TKE when the PFN emission stops for different mass values and plotted on the left side of the slide. Presented data are of great interest for comparison with theoretical calculations

Prompt fission neutron investigation

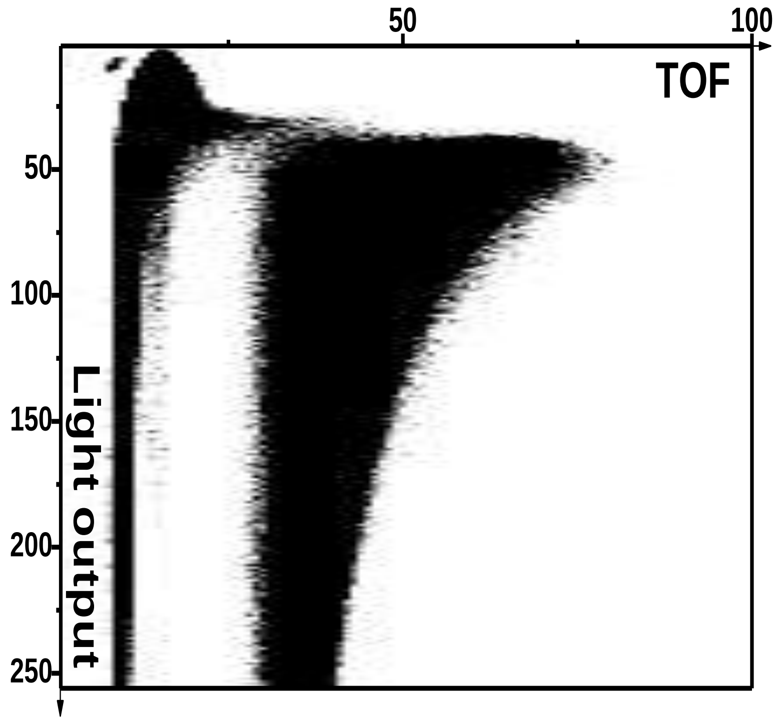

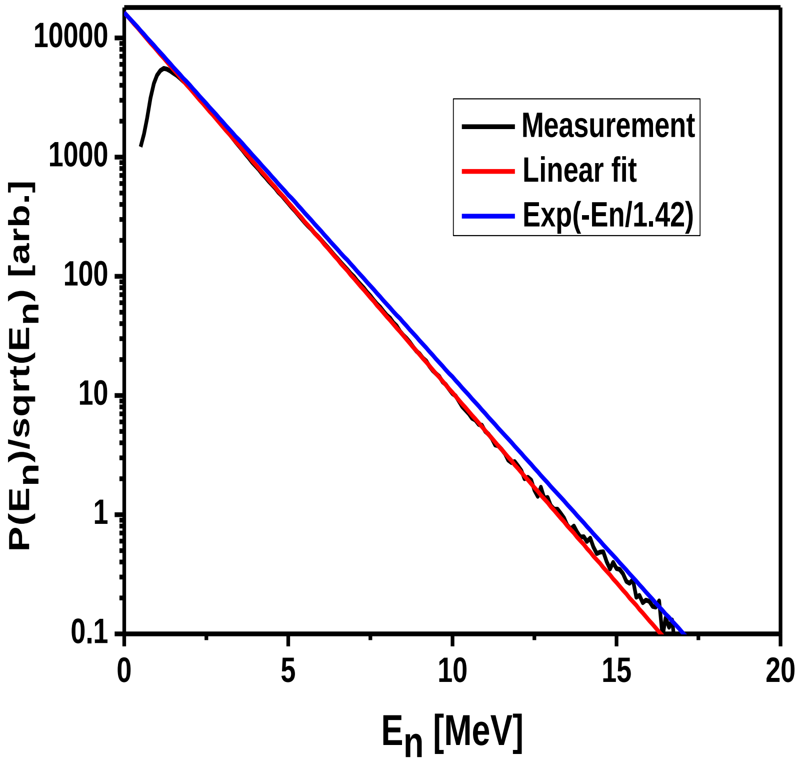

Another important parameter, which could be extracted from the experimental data is PFN spectral parameters.

Comparison of angular distributions

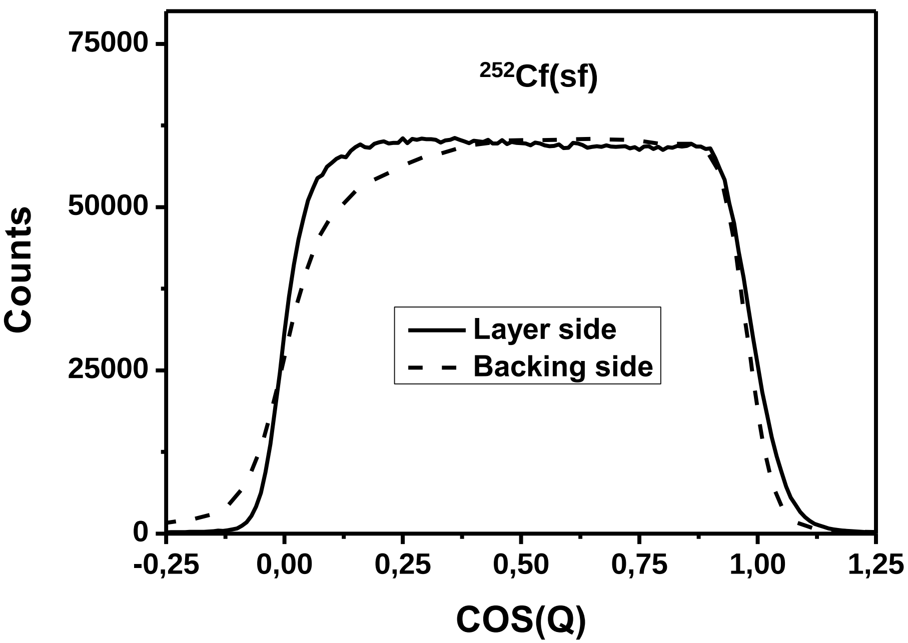

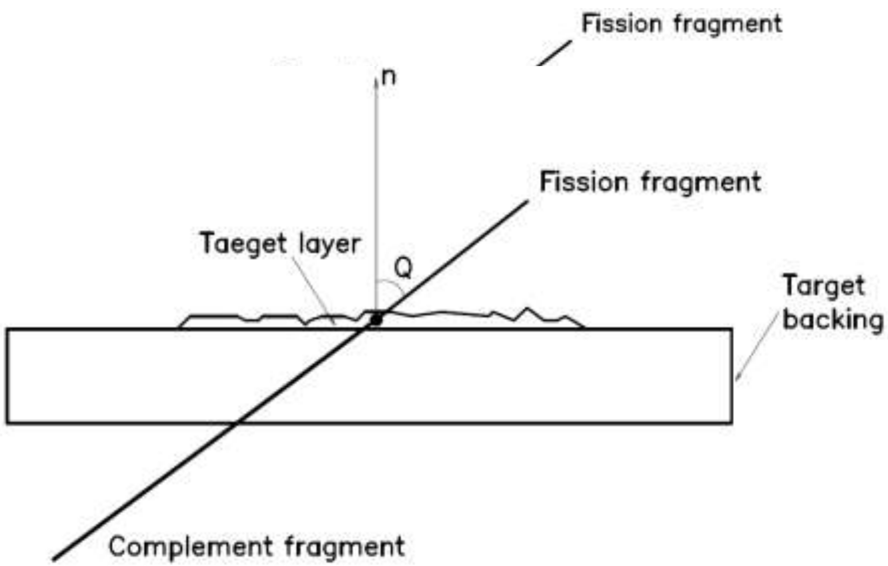

Angular distribution measured from the target layer side demonstrates rather better accuracy, almost independent on the FF angle in respect to the layer surface. The backing side accuracy degrades as the FF angle approaches 90◦. This fact complicates measurement of PFN emission for targets like ^{235}U and ^{239}Pu. To overcome that complicity we developed a position sensitive TIC, allowing measurement with an arbitrary allocated multiple ND

The Stripped Anode Ionization Chamber

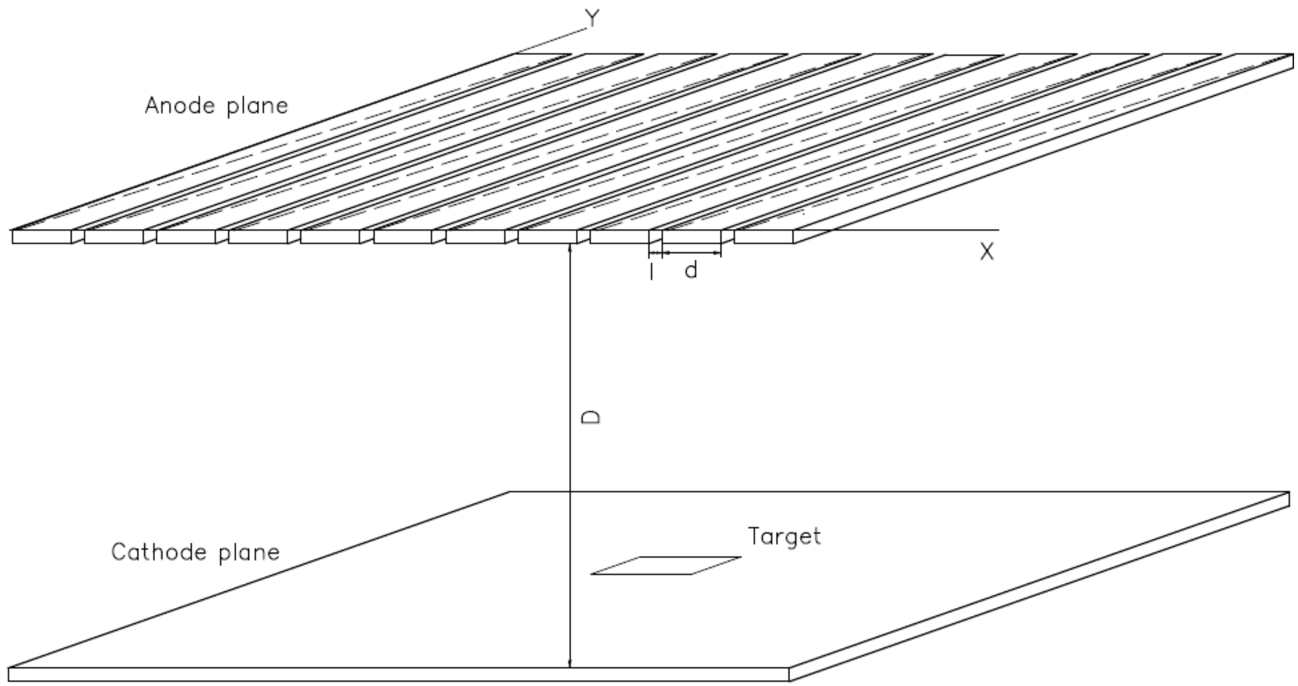

The anode of modified TIC was made of strips divided along the diagonal to make two isolated Δ-electrodes. Electrical contacts are made to each Δ-electrode. If no space charges are present in the chamber volume and if the dimensions of the chamber in the *x* and y directions are large compared with the thickness of strips, then edge effects can be neglected .

Signal formation in the ionization chamber

Signals from the TGIC anodes arise because of the motion of charge carriers after they are formed by the FF

The time evolution of the signal is of fundamental importance in understanding the timing properties of pulses as well as in predicting the effects of changes in the location of the radiation interactions on the shape of the pulse.

The Laplace equation with properly chosen boundary conditions is the starting point for these calculations

$$\nabla^2\varphi = 0, \text{ where } \nabla^2 = \frac{\partial^2}{\partial x^2} + \frac{\partial^2}{\partial y^2}, \ \text{Electric field } \varepsilon = -grad\varphi$$

In case of ionization chamber potential φ is linear function along the fission axis for the working area far enough from the side walls of the chamber. It would be worth to consider signal formation on the chamber electrodes using the Ramo-Shockley theorem.

To do that we have to find the weighting potential ϕ_0 as the solution of Laplace equation for the geometry of the detector with some artificial boundary conditions:

1. **The voltage on the electrode for which the induced charge is to be calculated is set equal to unity.**
2. **The voltages on all other electrodes are set to zero.**
3. **Even if a trapped charge is present within the detector volume, it is ignored in the calculation.**

$$\frac{\partial^2 F(x,y)}{\partial x^2} + \frac{\partial^2 F(x,y)}{\partial y^2} = 0$$

$$\frac{\partial^2 F}{\partial x^2} = \frac{2F_v}{v(v+q)} + \frac{2F_q}{q(q+v)} - \frac{2F_o}{qv}, \qquad \frac{\partial^2 F}{\partial y^2} = \frac{2F_p}{p(p+u)} + \frac{2F_u}{u(p+u)} - \frac{2F_o}{pu}$$

$$\frac{F_v}{v(v+q)} + \frac{F_q}{q(v+q)} + \frac{F_p}{p(p+u)} + \frac{F_u}{u(p+u)} = \frac{pu+qv}{puqv} F_o \quad \text{- finite difference Laplace equation}$$

Weighting potential for the single strip

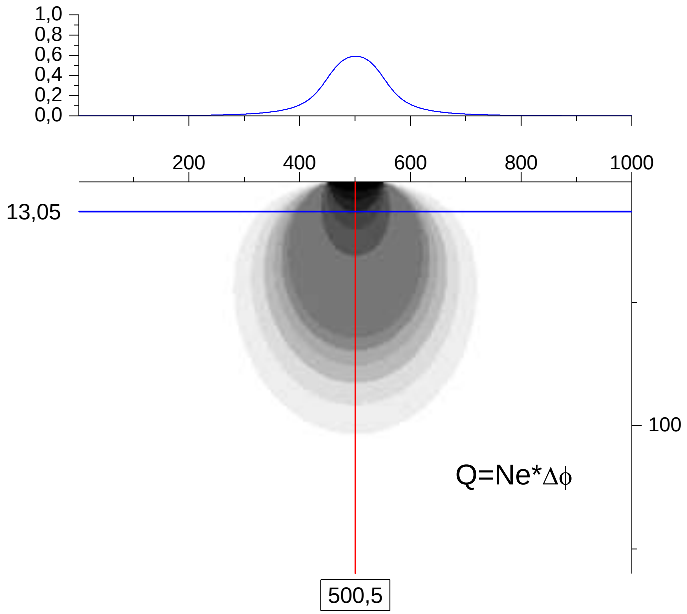

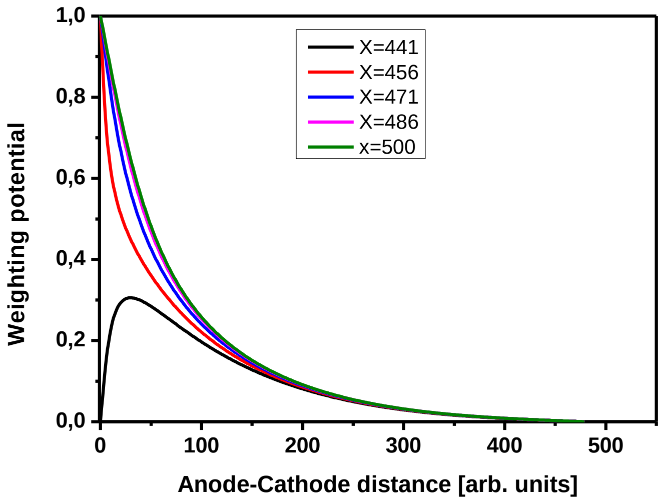

The weighting potential in the TIC volume was calculated for one strip potential raised to 1 leaving other electrodes grounded. If the strips are operated at positive potential relative to the cathode surface, then ionization electrons will be attracted along field lines that are parallel to each other and perpendicular to the anode surfaces. It is very important to notice that the only electrons that collected by the selected strip will contribute to the charge integrated on the strip circuit. But it does not mean that a potential will not be induced on selected strip by the electrons collected on neighbouring strips. It should be carefully taken into account in pulse processing electronics to minimize possible cross-talks between the strips.

Comparison with TGIC

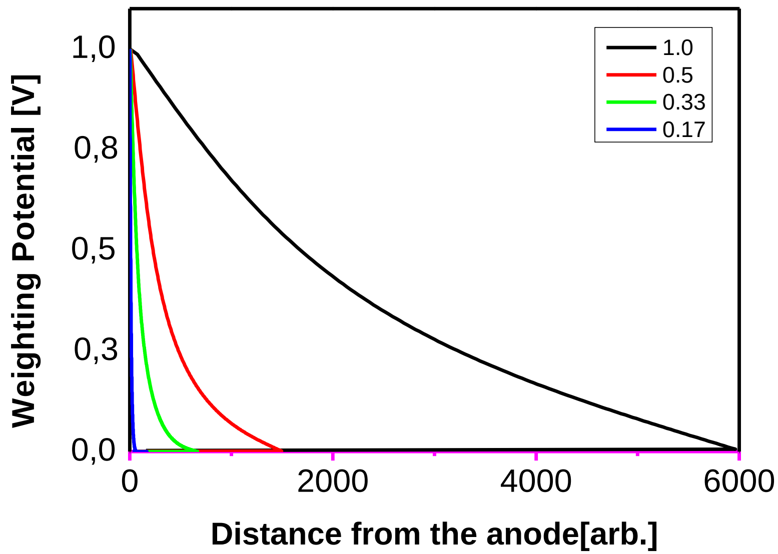

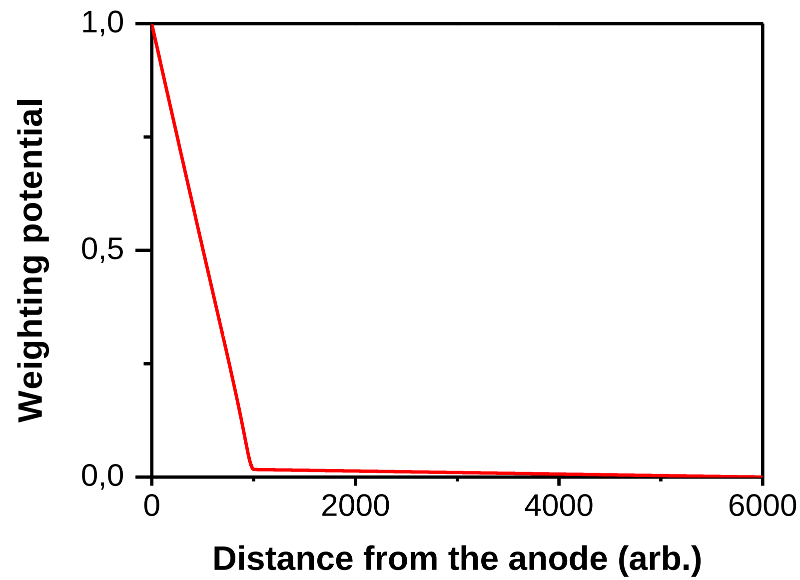

Left graph demonstrates the weighting potential dependence on the ratio of the anode strip width to the anode-cathode distance. On the right graph the weighting potential for Frisch-gridded IC is shown. Comparison demonstrates that if anode-cathode distance is properly chosen, then there is no need in Frisch-grid at all. This has influence on the pulse shape of individual strip and possibly could facilitate determination of ionization density along the fission fragment deceleration path. This effect has to be investigated. Apparently the new TIC has faster pulse rise time, making it more suitable in experiments with high intrinsic alpha-radioactive targets.

DPP electronics for position sensitive TIC

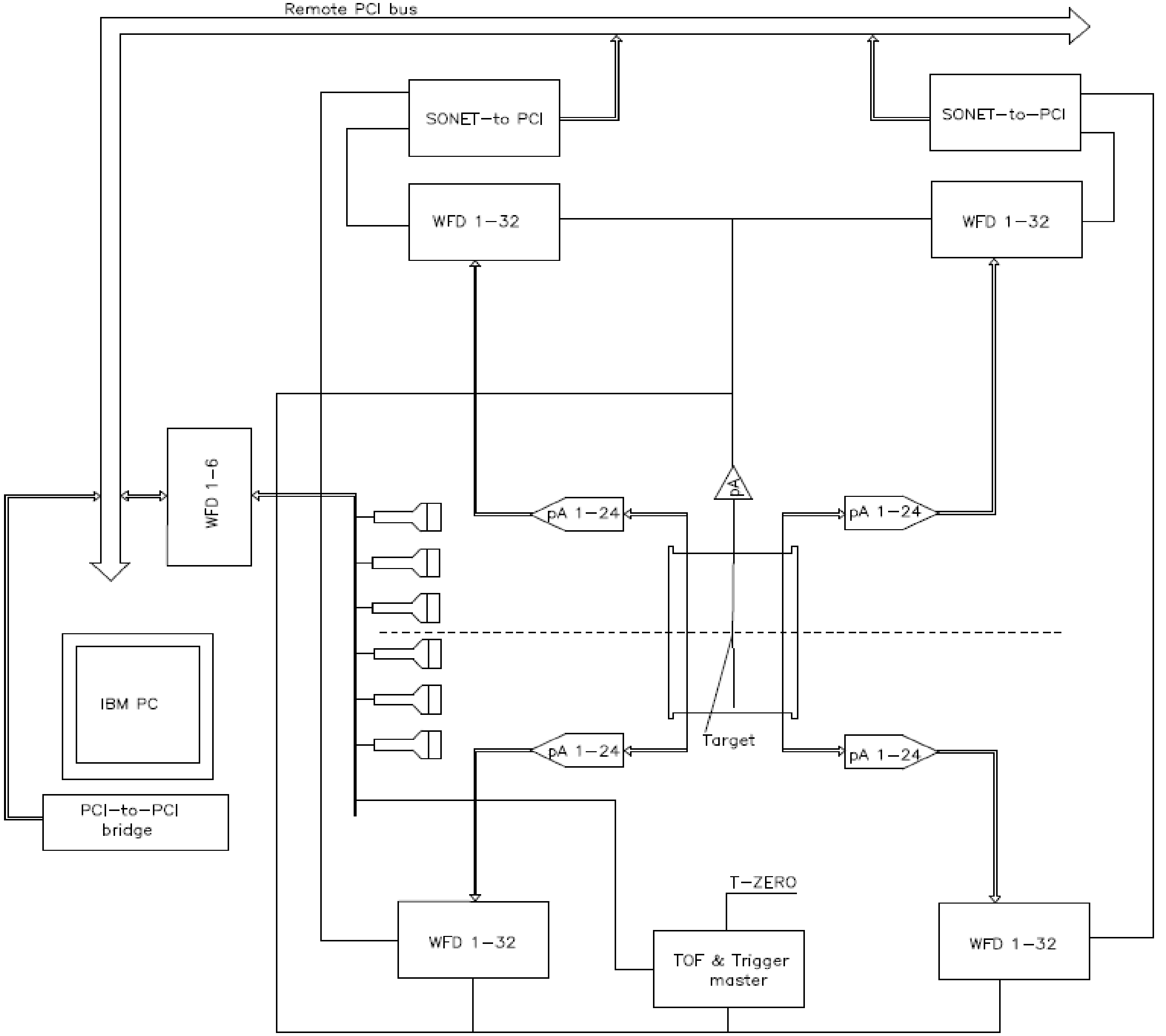

Prompt fission neutron investigation

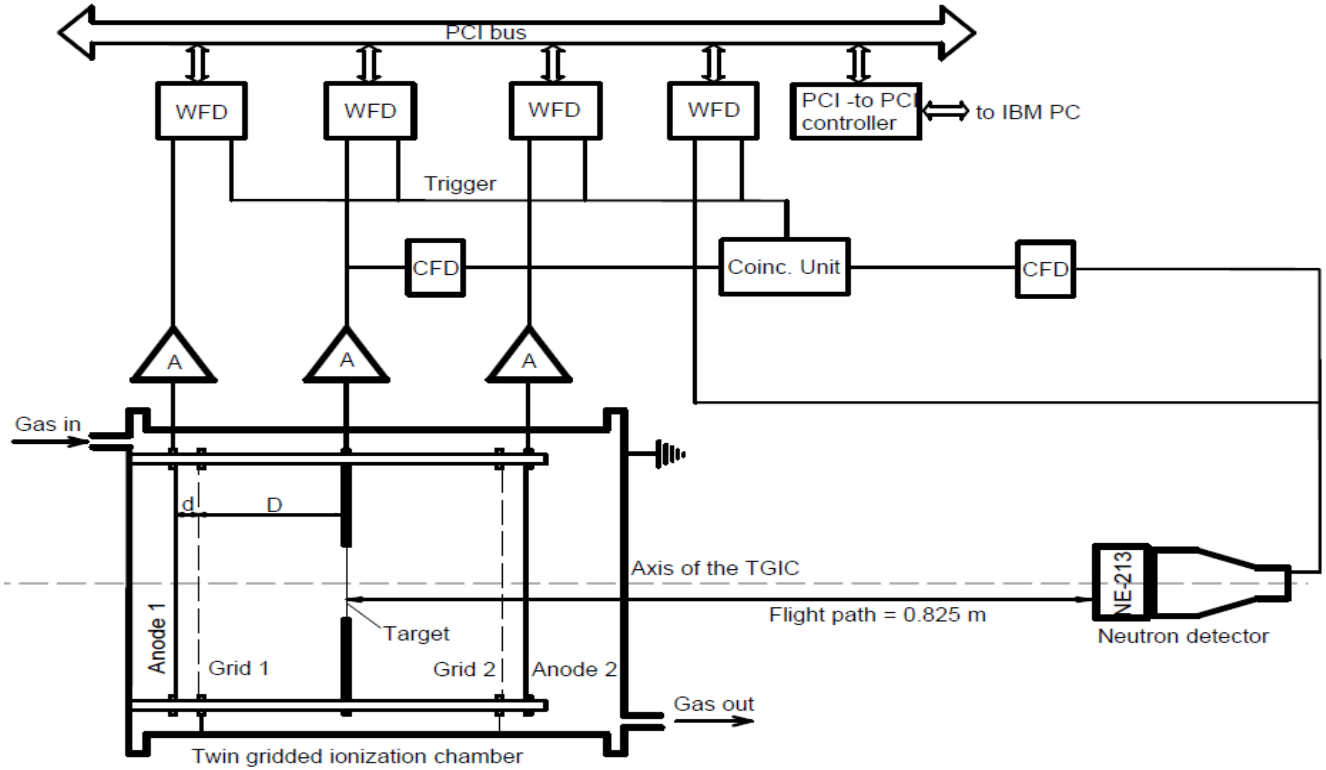

Constant fraction time triggering (CFTT) was implemented digitally to measure the time difference between TIC cathode and ND pulse. Additionally the TIC cathode pulse before CFTT was preprocessed using "differentiating" procedure realized by subtracting the waveform obtained by passing the original waveform trough a second order low pass filter from the original waveform.

DPP application to n-γ pulse shape separation

In our data analysis procedure two types of neutron/gamma separation algorithms were implemented. First one was based on integrating of ND current pulse over two different time periods (TIM). The second one is adopted from famous book ("Random DATA Analysis and Measurement Procedures" by J. Bendat and A. Piersol) and based on analysis of cross-correlation the ND waveform *N(t)* with the analytical function. The last function was approximately similar to ND response to gamma-radiation according to the following formula:

$$R(t) = A*(1-\exp(-t/T_1))*\exp(-t/T_2)$$

where A, T_1, T_2 were fitting parameters. The cross-correlation function (CCF) was calculated according to formula:

$$CCF(k*\Delta) = \sum_i R(i*\Delta)N((k+i)*\Delta)$$

Where functions *CCF(t), R(t)* and *N(t)* were sampled in homogeneously distributed intervals of width Δ and k, i are indexes running from 0 to N – total number of waveform samples. CCF was calculated event by event and its "centre-of-gravity" value-*G*, calculated according to formula:

$$G = \frac{\sum_i i*CCF(i*\Delta)}{\sum_i CCF(i*\Delta)}$$

Two integral method (TIM)

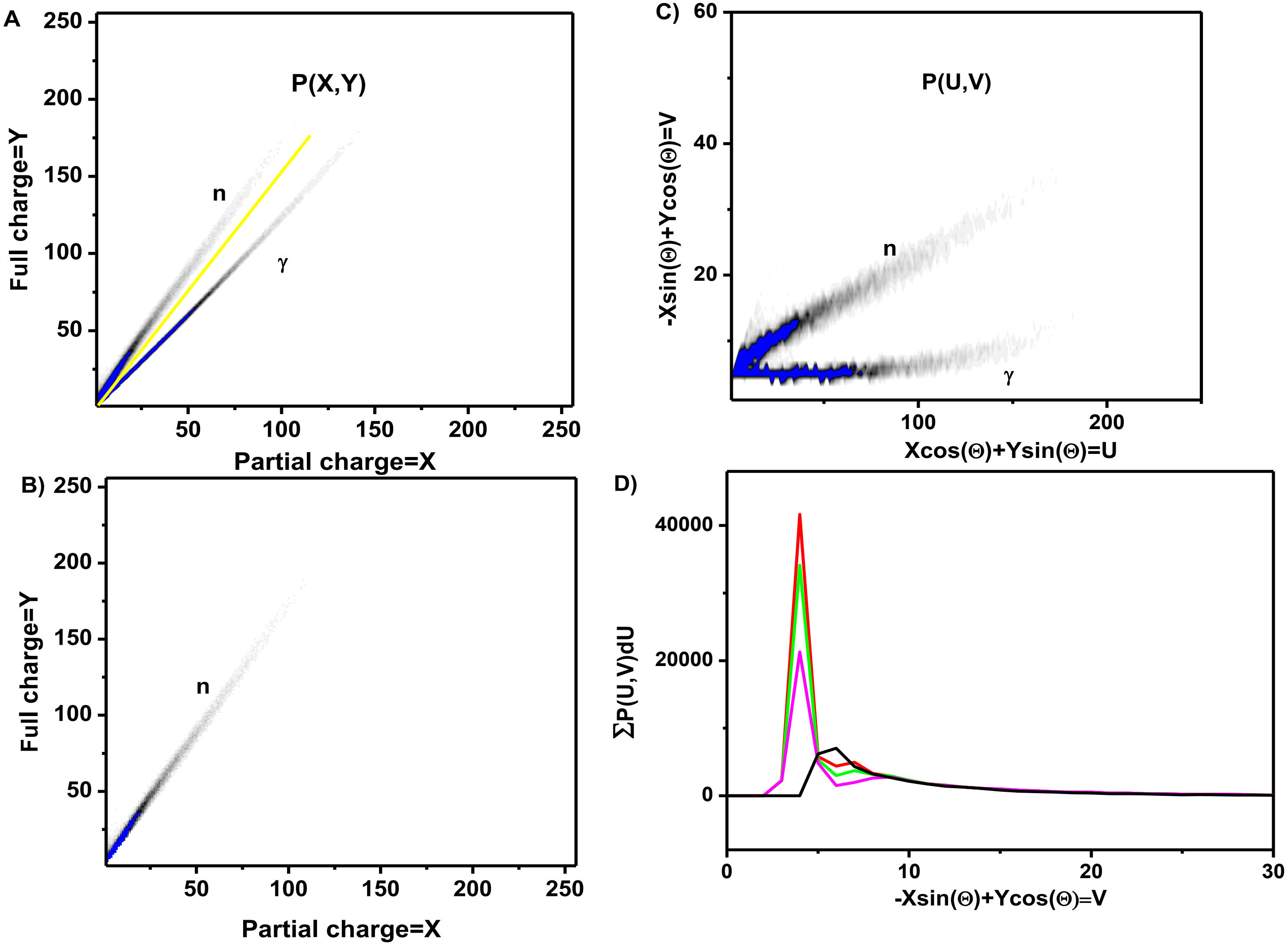

Prompt fission neutron investigation

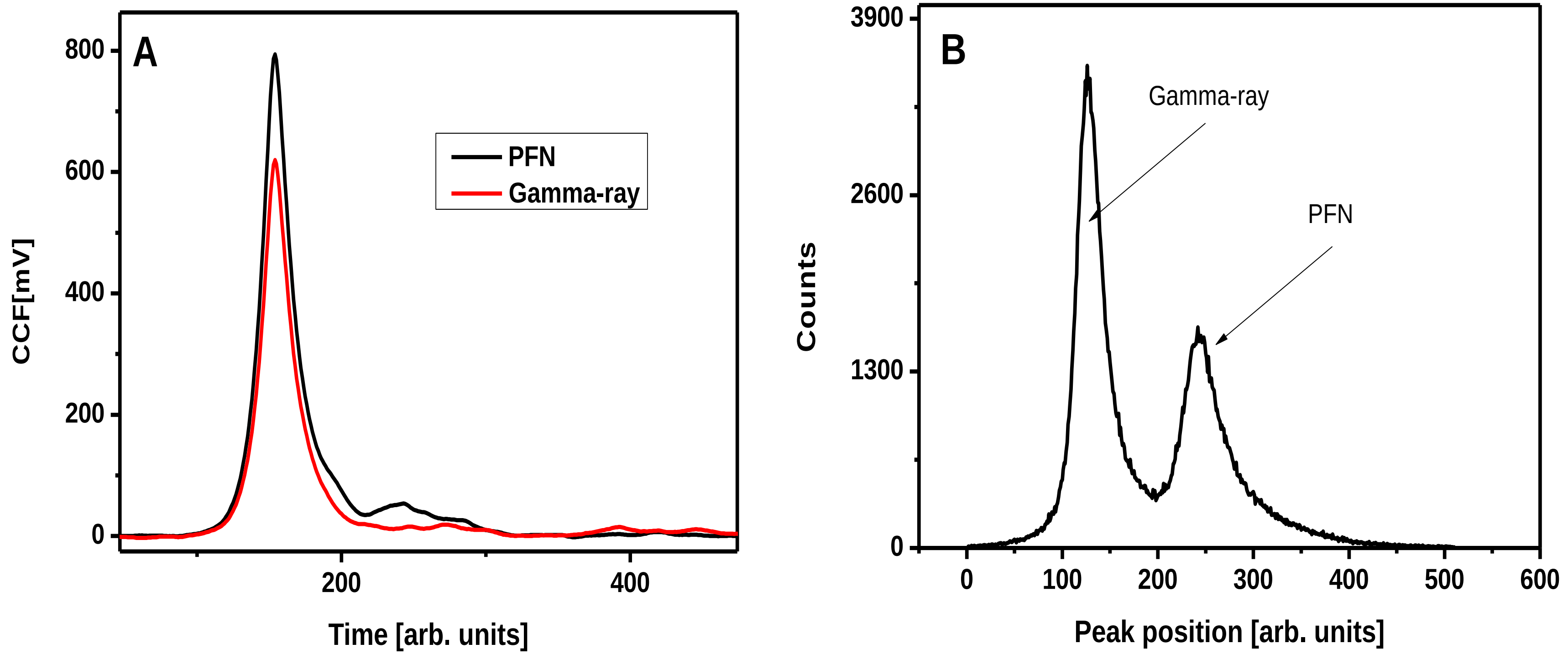

Fig. A demonstrates typical neutron and gamma response of ND. Fig. B demonstrates distribution of "gravity centre of CCF", calculated event by event in ^{252}Cf(SF) .

Two peak distribution demonstrates very good n-γ separation when events selected with properly chosen "Peak position" parameter.

Prompt fission neutron investigation

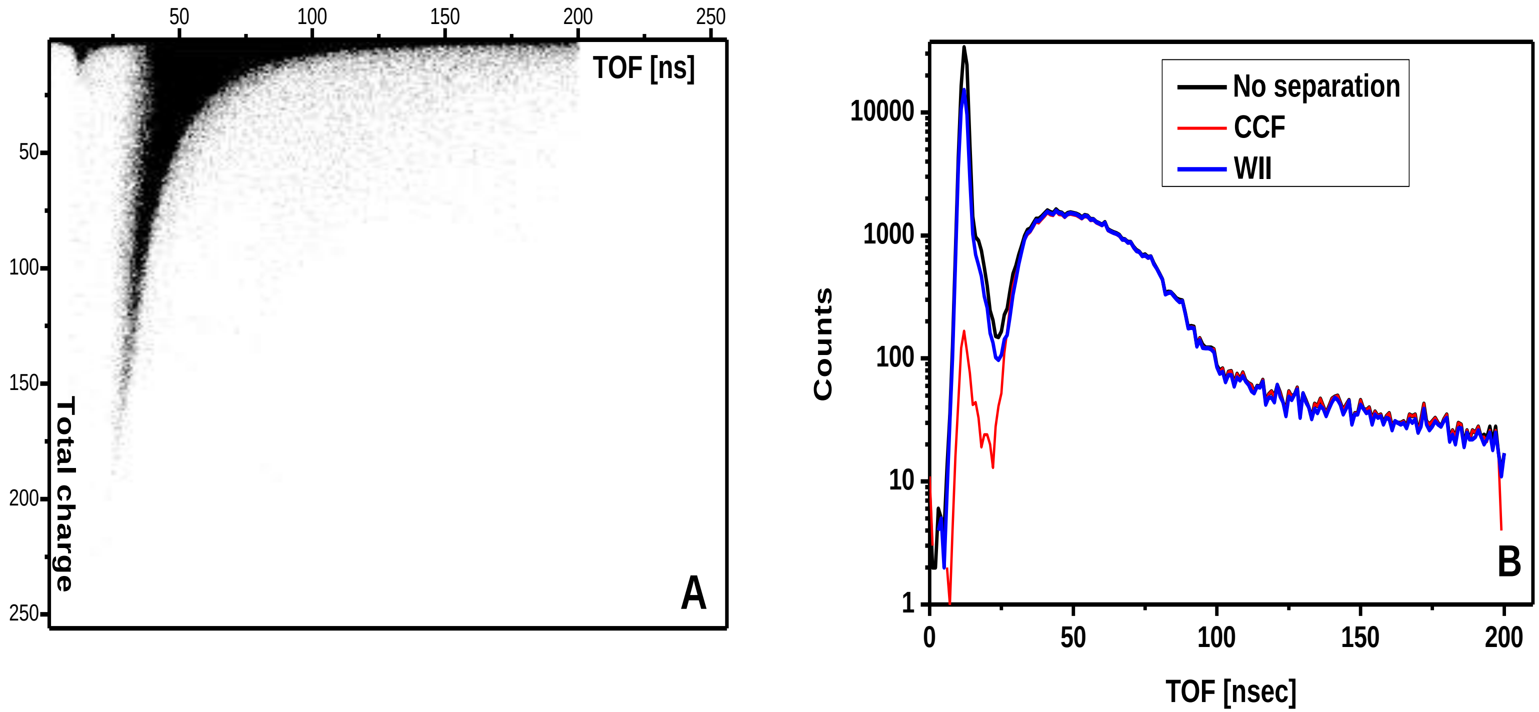

Fig. B demonstrates PFN TOF distribution plotted without application of any n-γ separation (black), applying TII (blue) and CCF (red) lines. CCF curve was plotted for “Peak position” parameter chosen exactly in the middle between peaks. Fig. A demonstrates two-dimensional plot in coordinates (**Total charge,TOF)** created for the same events as used for CCF curve in the Fig. B. Two factors of magnitude greater γ-suppression factor was achieved in comparison with simple TII method. As it was noticed before TII method could be improved to provide comparable results.

Summary and conclusions

Design of position sensitive ionization chamber utilizing backgammon principle was presented along with DPP and main formulas necessary for data analysis. DPP algorithms are basically the same as for gridded IC due to position sensitive chamber can be considered as many “Frisch-gridded” IC working in parallel, but having independent pulse processing electronics.

The chamber was designed to be suitable for FF mass@TKE spectroscopy and PFN emission kinematics reconstruction. We hope that TIC will provide the new quality of PFN investigation with multiple fast neutron detectors.

A new detector can be used in neutron imaging applications as a competitive option to existing solutions.

PFN detection was considered with focus on optimization of DPP algorithms for both TOF and pulse shape analysis using the benefits provided by digitizers.

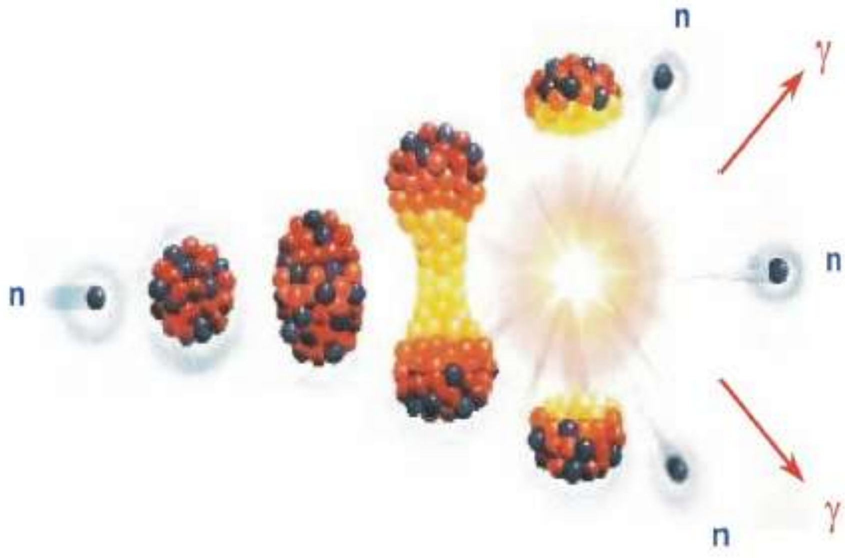

Thank you for your attention ☺